IEEE Access
Multidisciplinary | Rapid Review | Open Access Journal

Received July 13, 2018, accepted August 23, 2018, date of publication August 28, 2018, date of current version September 21, 2018.

Digital Object Identifier 10.1109/ACCESS.2018.2867463

Adaptive Nonsingular Terminal Sliding Model Control for Permanent Magnet Synchronous Motor Based on Disturbance Observer

BO XU, XIAOKANG SHEN, WEI JI, GUODING SHI, JIAN XU, AND SHIHONG DING
School of Electrical and Information Engineering, Jiangsu University, Zhenjiang 212013, China

Corresponding author: Wei Ji (jwhxb@163.com)

This work was supported in part by the National Natural Science Foundation of China under Grant 61703186, in part by the Natural Science Foundation of Jiangsu Province under Grant BK20150530, in part by a project funded by the Priority Academic Program Development of Jiangsu Higher Education Institutions, and in part by the Professional Research Foundation for Advanced Talents of Jiangsu University under Grant 14JDG077.

ABSTRACT In order to shorten the response time and improve robustness for a permanent magnet synchronous motor (PMSM) control system, an adaptive nonsingular terminal sliding model control (NTSMC) equipped with a disturbance observer is presented for PMSM. First, an improved exponential reaching law is adopted to adaptively adjust exponential and constant approach speed in the adaptive NTSMC. Second, the disturbance observer is devised to observe the load torque and external disturbance and feeds back them to the adaptive NTSMC to compensate. Simulation and experimental results applied to PMSM show that the proposed approach can quickly track load torque and external disturbance and the system has advantages of small overshoot, static error, rapidity, and higher robustness.

INDEX TERMS PMSM, adaptive NTSMC, disturbance observer.

I. INTRODUCTION

PMSM (Permanent Magnet Synchronous Motor) has characteristics of simple structure, small size, less weight, high efficiency, high factor, rotor heat out of question, better over loading, lesser moment of inertia and torque ripple. It has been widely used in the fields of numerical control machine tools, medical instruments, instruments and meters, aviation and spaceflight. It is well known that traditional control schemes, such as PID (proportion integral derivative), are already widely used in the PMSM control system due to its simple implementation [1]. However, the PMSM system is the nonlinear, time-varying and complex with unavoidable and unmeasured disturbances as well as parameter variations. It is very difficult to achieve a satisfactory performance in the entire operating range only by using traditional control algorithm [2]–[5].

In recent years, various modern control techniques have been presented to improve the different aspects performance of the PMSM control system [6]–[12]. Among these methods, the sliding mode control (SMC) method is considered to be efficient to increase the disturbance rejection and the robustness property of the PMSM system and have been improved in intensive studies [13]–[16]. To further improve the dynamic performance of the SMC, a direct method is to introduce the nonlinear sliding surfaces. Terminal sliding mode (TSM), as one of nonlinear sliding surfaces, can ensure the finite-time convergence [17], [18]. The TSM control method with the nonlinear term can guarantee system converge on a specified trajectory in finite time. In order to solve singular problem, [19] presented the nonsingular terminal sliding model control. Reference [20] adopted new reaching law to design control law. This method not only improved system response but also reduced chattering effectively. Reference [21] designed variable-rated exponential reaching law, but the method didn't consider the selection of reaching law when state variable is close to zero.

In our previous study [22], the L_1 norm of state variable was used to design adaptive variable-rated exponential reaching law. However, the problems of system uncertainty and external disturbance weren't considered. In this paper, based on [22] and [23], an improved exponential reaching law is present to design control law. In order to shorten the reaching time and weaken system chattering, exponential and constant approach speed can adaptively adjust to the equilibrium position in accordance with the distance of state variables. In additional, in terms of system uncertainty,

external disturbance and load torque, according to the basic idea of disturbance observer which can estimate disturbances and feedback them to foreword channel immediately to compensate [24], [25]. This paper designs the disturbance observer (DOB) on basis of the theory of Luenberger state observer instead of taking the boundary value. The proposed disturbance observer can observe the values of load torque, system uncertainty and external disturbance in real time, and then feed back them to the sliding model controller. This method extracts the advantages of the adaptive NTSMC and the disturbance observer, which not only shortens the reaching time and weakens system chattering, but also improves system robustness. The application of the proposed approach in a simulation and engineering system indicate its validity.

II. MATHEMATICAL MODEL OF PMSM

In order to simplify analysis, in this paper, the PMSM stator adopts three-phase symmetrical windings, and the rotor has a permanent magnet structure. Assuming that the magnetic field is sinusoidally distributed in space, without considering the effects of hysteresis and eddy current loss, take the d axis in line with the excitation axis of the permanent magnet, and the q axis follows the direction of rotation of the rotor and leads the d axis $\pi/2$ electrical angle. Mathematical model of magnetic synchronous motor in d-q coordinate system ($L_d = L_q = L$ for surface mounted PMSM) as follows [26].

$$\begin{cases} u_d = Ri_d - \omega_r L_q i_q + L_d \dfrac{di_d}{dt} \\ u_q = Ri_q + \omega_r L_d i_d + L_q \dfrac{di_q}{dt} + \omega_r \psi \end{cases} \tag{1}$$

where u_d, u_q, i_d and i_q are stator voltage and current components in the d-q coordinate system respectively; L_d, L_q are respectively inductances on d axis and q axis; R points motor winding resistance; ω_r indicates the electric angular velocity; and ψ presents the flux of permanent magnet.

The torque equation of PMSM is:

$$T_e = 1.5p[\psi i_q + (L_d - L_q) i_d i_q] \tag{2}$$

where T_e is the electromagnetic torque; and p refers to pole pairs. For the surface PMSM,$L_d = L_q = L$, thus the torque equation is reduced to as follows:

$$T_e = 1.5p\psi i_q \tag{3}$$

The motion equation of PMSM is:

$$T_e - T_L - F\omega = J\frac{d\omega}{dt} \tag{4}$$

where T_L is load torque; ω points the mechanical angular velocity of the motor; F means friction coefficient of the rotor and load; and J implies inertia moment.

The following equation considers the uncertainty of the PMSM system.

$$\begin{aligned} \frac{d\omega}{dt} &= \left(\frac{1.5p\psi}{J} + \Delta a\right) i_q - \left(\frac{F}{J} + \Delta b\right)\omega - \left(\frac{1}{J}T_L + \Delta d\right) \\ &= \frac{1.5p\psi}{J} i_q - \frac{F}{J}\omega - \frac{T_L - Ji_q\Delta a + J\omega\Delta b + J\Delta d}{J} \\ &= \frac{1.5p\psi}{J} i_q - \frac{F}{J}\omega - \frac{g(t)}{J} \end{aligned} \tag{5}$$

where $g(t) = T_L - Ji_q\Delta a + J\omega\Delta b + J\Delta d$.

III. DESIGN OF THE ADAPTIVE NTSMC

A. SLIDING SURFACE

$$\begin{cases} x_1 = \omega^* - \omega \\ x_2 = \dot{x}_1 = -\dot{\omega} \end{cases} \tag{6}$$

Equation (7) is obtained from equation (5) and equation (6):

$$\begin{aligned} \dot{x}_2 &= -\ddot{\omega} \\ &= -\frac{F}{J}x_2 - \frac{1.5p\psi}{J}\dot{i}_q + \frac{\dot{g}(t)}{J} \end{aligned} \tag{7}$$

Assuming that $g(t)$ is the total uncertainty, thus there is the following equation:

$$g(t) = T_L - Ji_q\Delta a + J\omega\Delta b + J\Delta d \tag{8}$$

From equation (6), (7) and (8), the speed error state equations can be presented as follows:

$$\begin{cases} \dot{x}_1 = x_2 \\ \dot{x}_2 = -\dfrac{1.5p\psi}{J}\dot{i}_q - \dfrac{F}{J}x_2 + \frac{\dot{g}(t)}{J} \end{cases} \tag{9}$$

For system (9), in order to achieve excellent performance, the nonsingular terminal sliding surface is designed as follows:

$$s = x_1 + \frac{1}{\beta}x_2^{p/q} \tag{10}$$

where $\beta > 0$, p and q are positive odd integers under the situation of $1 < p/q < 2$.

B. CONTROL LAW

For system (9), the ordinary exponential reaching law is adopted to design the SMC. The reaching law is as follow:

$$\dot{s} = -\varepsilon \mathrm{sgn}(s) - ks, \quad \varepsilon > 0 \tag{11}$$

The reaching law includes the index reaching item $-ks$, and the constant rate reaching item $-\varepsilon\mathrm{sgn}(s)$. In equation (11), k and ε are constant and not self-adaptive, so system convergence characteristics cannot achieve the best performance for different position state variables. In here, an adaptive variable rate exponential reaching law is present by the following:

$$\dot{s} = -\varepsilon\frac{1}{1 + c\|x\|_1}\mathrm{sgn}(s) - (k + c\|x\|_1)s \tag{12}$$

where, $k > 0, \varepsilon > 0, c > 0$, and $\|x\|_1 = \sum_{i=1}^{n} |x_i|$ is the first-order norm of state variables of the system, $n > 0$.

The adaptive variable-rated exponential reaching law (12) introduced the first-order norm of state variables can adaptively adjust its exponential approach speed and constant approach speed. The instant result of exponential reaching item is $s = s(0)e^{-(k+c\|x\|_1)t}$ for equation (12). When $\|x\|_1$ is large and the exponentially decaying speed is much greater than that in equation (11), the reaching time can be greatly shortened. Meantime, the reaching rate $\varepsilon\frac{1}{1+c\|x\|_1}$ of constant rate reaching item is far less than ε of equation (11). When $\|x\|_1$ is small, by increasing the adjustment coefficient c, the reaching time of the sliding mode can be shortened and system chattering can be weakened. When the selected state variable x converges to zero, the adaptive variable-rated exponential reaching law will decrease to the constant index reaching law.

In the consideration of the speed error state equation (9), the sliding surface equation (10) and the reaching law (12), the PMSM control law can be designed as follows:

$$i_q = \frac{J}{1.5p\psi}\left\{\int_0^t\left[-\frac{F}{J}x_2+\beta\frac{q}{p}x_2^{2-\frac{p}{q}}+\varepsilon\frac{1}{1+c\|x\|_1}\mathrm{sgn}(s)+(k+c\|x\|_1)s\right]dt+\frac{g(t)}{J}\right\} \tag{13}$$

C. STABILITY ANALYSIS

Choosing Lyapunov function:

$$V=\frac{1}{2}s^2 \tag{14}$$

and taking the derivative of sliding surface (10) along system (9):

$$\dot{s}=\dot{x}_1+\frac{1}{\beta}\frac{p}{q}x_2^{\frac{p}{q}-1}\dot{x}_2=x_2+\frac{1}{\beta}\frac{p}{q}x_2^{\frac{p}{q}-1}\dot{x}_2 \tag{15}$$

Then

$$\begin{aligned}\dot{V}&=s\dot{s}=s\left(x_2+\frac{1}{\beta}\frac{p}{q}x_2^{\frac{p}{q}-1}\dot{x}_2\right)\\&=\frac{1}{\beta}\frac{p}{q}x_2^{\frac{p}{q}-1}\left\{s\left[g(t)-l_g\mathrm{sgn}(s)\right]-\varepsilon\frac{1}{1+c\|x_1\|}|s|-(k+cx_1)s^2\right\}\end{aligned} \tag{16}$$

Two different cases will be discussed as follows:

(1) When $x_2\neq 0$

$$\dot{V}=s\dot{s}\le\frac{1}{\beta}\frac{p}{q}x_2^{\frac{p}{q}-1}\left\{-\varepsilon\frac{1}{1+c\|x_1\|}|s|-(k+cx_1)s^2\right\}\le 0 \tag{17}$$

In this case, the system will converge to zero in finite time.

(2) When $x_2=0$

$$\dot{x}_2=g(t)-l_g\mathrm{sgn}(s)-\varepsilon\frac{1}{1+c\|x_1\|}|s|-(k+cx_1)s \tag{18}$$

Then

$$\begin{cases}\dot{x}_2\le-\varepsilon\dfrac{1}{1+c\|x_1\|}, & s>0\\ \dot{x}_2\ge\varepsilon\dfrac{1}{1+c\|x_1\|}, & s<0\end{cases} \tag{19}$$

It is can be seen from equations in (18) that, when $s>0$ and $x_2=0$, x_2 is not in steady state and will change into $x_2<0$ in finite time. Besides, the sliding mode surface will be achieved in finite time, which can be proved in the case of $x_2\neq 0$. Similarly, when $s<0$ and $x_2=0$, x_2 is not in steady state and will change into $x_2>0$ in finite time. At the same time, the system will reach the sliding mode surface from initial state in finite time.

The results show that in a limited time, the sliding mode can be obtained anywhere in the phase plane.

IV. DISTURBANCE OBSERVER

A. DESIGN OF DISTURBANCE OBSERVER

It can be seen from the control law (13) that $g(t)=T_L-Ji_q\Delta a+J\omega\Delta b+J\Delta d$ is an unknown quantity and cannot be measured. In this paper, the disturbance observer is designed to observe the values of disturbance and load torque in real time.

ω can be measured and $\frac{d\omega}{dt}=\frac{1.5p\psi}{J}i_q-\frac{F}{J}\omega-\frac{g(t)}{J}$. The disturbance observer can be designed by the theory of Luenberger liner observer.

The PMSM speed system can be presented as follows:

$$\begin{cases}\dot{x}=Ax+Bu\\ y=Cx\end{cases} \tag{20}$$

where state variable $x=\left[\omega\ g(t)\right]^T$, output variable $y=\omega$, input variable $u=1.5p\psi i_q$, $A=\begin{bmatrix}-\frac{F}{J} & -\frac{1}{J}\\ 0 & 0\end{bmatrix}$, $B=\left[\frac{1}{J}\ 0\right]^T$ and $C=\left[1\ 0\right]$.

It can be known from the modern control theory that (A, C) is observable, thus the state observer exists.

Constructing the state observer for system (20)

$$\begin{cases}\dot{\hat{x}}=A\hat{x}+Bu+L\left(y-\hat{y}\right)\\ \hat{y}=C\hat{x}\end{cases} \tag{21}$$

where $\hat{x}=\left[\hat{\omega}\ \hat{g}(t)\right]$ is the estimated value of x, $\hat{y}$ is the estimated value of y, and $L=\left[l_1\ l_2\right]$ points the feedback matrix.

The error equation of this observer is as the following:

$$\dot{e}=\dot{x}-\dot{\hat{x}}=(A-LC)e \tag{22}$$

For equation (22), if the eigenvalues of matrix $(A-LC)$ all have negative real parts, the state error e will converge to zero asymptotically. The poles of equation (22) should be placed in the left half plane through pole assignment to ensure the system error converging to zero.

Substituting $\hat{g}(t)$ into equation (13) obtains the following equation:

$$i_q=\frac{J}{1.5p\psi}\left\{\int_0^t\left[-\frac{F}{J}x_2+\beta\frac{q}{p}x_2^{2-\frac{p}{q}}+\varepsilon\frac{1}{1+c\|x\|_1}\mathrm{sgn}(s)+(k+c\|x\|_1)s\right]dt+\frac{\hat{g}(t)}{J}\right\} \tag{23}$$

B. SIMULATION

In order to verify whether the disturbance observer can track the change of load and external disturbance, some simulated experiments are carried out. According to [22], the parameters of the adaptive NTSMC are $\beta = 1000$, $p = 9$, $q = 7$, $k = 45$,$\varepsilon = 80$ and $c = 50$. Fig.1 and Fig.2 show the results.

It can be seen from Fig.1 and Fig.2 that, when $g(t) = -5$, $g(t)$ estimation can make response to changes quickly and the error between $g(t)$ and $g(t)$ estimation is close to zero. When $g(t) = 0.05\sin(t)$, $g(t)$ estimation can track it quickly and exactly.

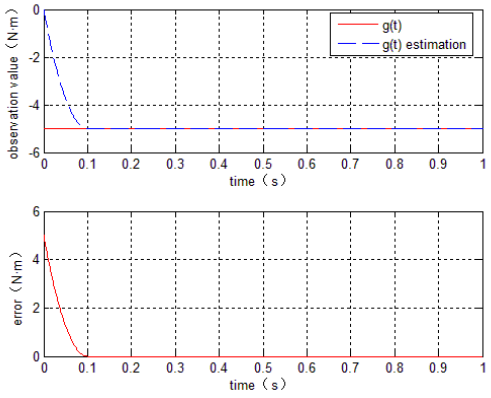

FIGURE 1. Fixed load observation and error.

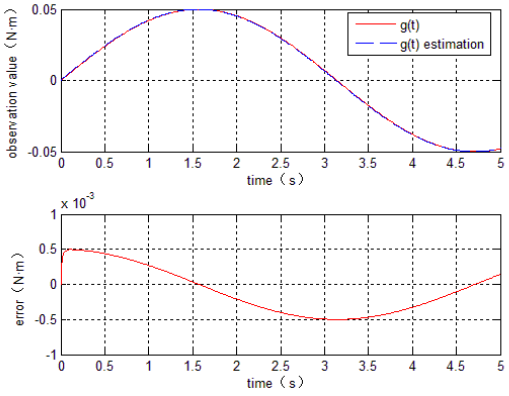

FIGURE 2. Dynamic load observation and error.

V. EXPERIMENTAL ANALYSIS

To verify the effectiveness of the designed controller, there is a hardware control system based on TMS320F28335 DSP for PMSM. The field-oriented control of $i_d = 0$ is adopted in this system. Fig.3 is the PMSM speed control system structure. Fig.4 shows the PMSM experimental platform. Specific parameters of PMSM are as follows: $L_d = L_q = 6.55mH$, $R = 0.901\Omega$, $\psi = 0.031Wb$, $p = 4$ and $J = 1.2 \times 10^{-4}kg \cdot m^2$. SVPWM is included in the whole algorithm, which is carried out in the program of the fixed point DSP TMS320F28335 under 100 MHz clock frequency. The utilization of C-program applies the control algorithm.

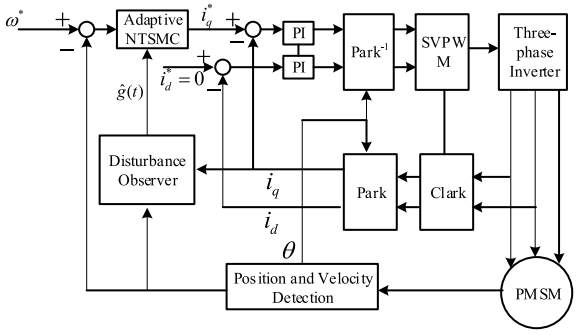

FIGURE 3. The PMSM speed control system structure.

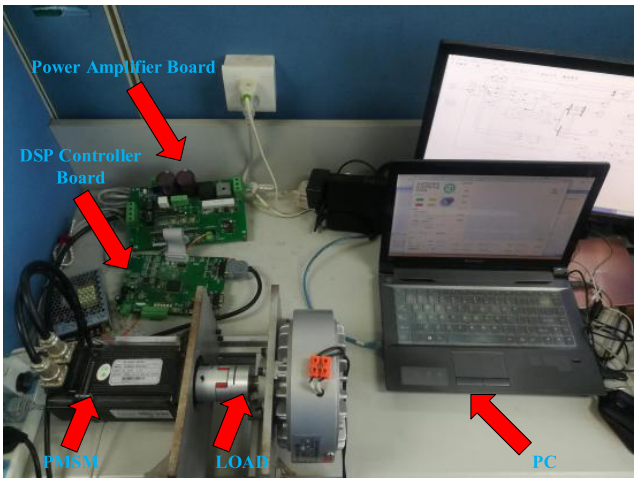

FIGURE 4. PMSM experimental platform.

The q axis reference current's saturation limit is ±8A. A three-phase voltage source PWM inverter is used to drive PMSM. This takes the advantage of IPM (intelligent power module) PS21865. The Hall-effect device is used to measure the phase currents. Meanwhile, the currents then are converted through the two 12-bit A/D converters. A SK-1A controller and a CZF25-eddy current brake are included in the AC speed regulation system to produce the braking torque, which can be applied as the external load disturbance. Afterwards, the tuning excitation current can be used to regulate the output torque of eddy current brake. Here, excitation current is set as 0.5A with external torque equal to rated load. The control gains of both current-loops are set as $k_p = 3$ and $k_i = 5$. The parameters of the adaptive NTSMC are the same as those in simulation.

With the help of dual system, the feedback matrix L of disturbance observer can be obtained: $L = [-7\ 12J - J^2]$. Fig.5 shows the effect of disturbance observer for torque when the given torque value changes from 0 to 3.2 $N \cdot m$. The experimental result shows that the proposed disturbance observer can track the actual value precisely in real time.

Fig.6 shows that the single phase current of the PMSM without load at speed of 1200r/min under the control of adaptive NTSMC with DOB. Additionally, Fig.7 shows the

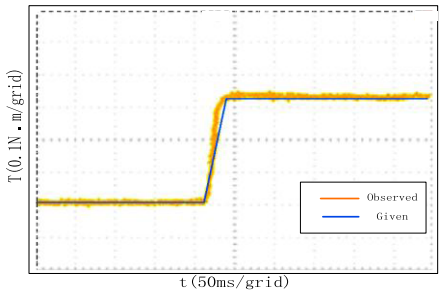

FIGURE 5. Observed value of disturbance observer.

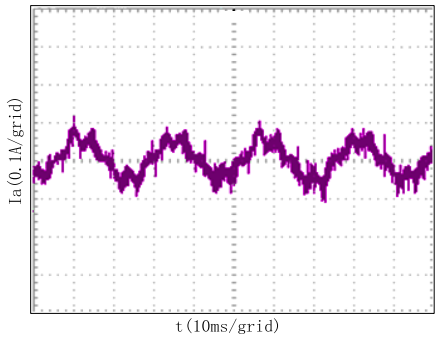

FIGURE 6. Current without load.

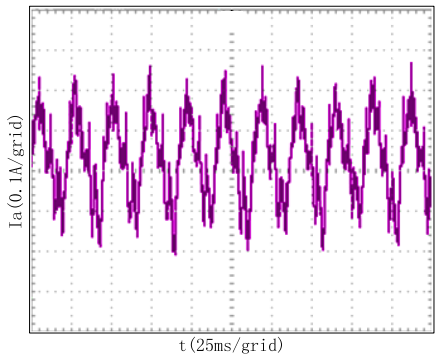

FIGURE 7. Current with load.

single phase current of the PMSM with the load of $3.2N \cdot m$. It can be seen the current presents a sine wave and is relatively stable.

Fig.8 shows the speed step response curve under the adaptive NTSMC with DOB and the NTSMC control. It can be seen clearly from Fig.8 (a) that, when PMSM speed is set as 1200r/min, the adaptive NTSMC with DOB response is 68.85%, faster than that of NTSMC control with only 2.3% overshoot. Fig.8 (b) shows that, when speed is set as 600r/min, the adaptive NTSMC with DOB response is 68.75% faster with smaller overshoot of just 2.17%. Fig.8 (c) shows that the adaptive NTSMC with DOB response is 42.86% faster with smaller overshoot of just 0.42% when speed is set as 300r/min. It can be concluded from these experimental results that the adaptive NTSMC with DOB can deliver faster speed response during start-up under the

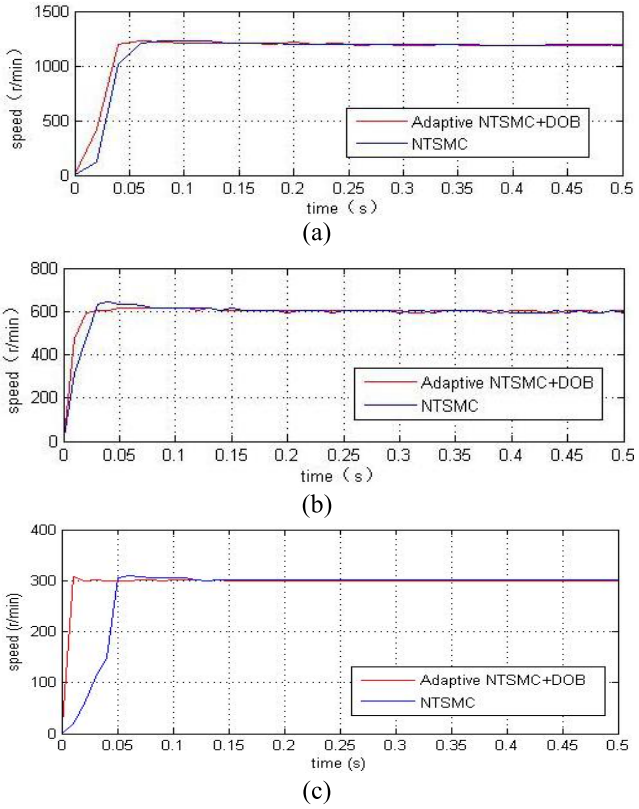

FIGURE 8. Speed step responses under the control of the adaptive NTSMC with DOB and NTSMC (a) 1200r/min. (b) 600r/min. (c) 300r/min.

comparison with NTSMC. Fig.9 shows the torque response without adding load when the target speed is 1200, 600, 300 r/min respectively. It can be clearly seen from figures that adaptive NTSMC with DOB has a fast torque response with smaller overshoot and chattering.

Fig.10 shows the speed response curve with a sudden change of speed from 1200r/min to 300r/min under the two controllers. It can be seen clearly that the adaptive NTSMC with DOB has less overshoot of only 4.33% and better velocity response, because it just uses 3ms to drop to 300r/min, but is 40% faster than NTSMC. Fig.11 displays the speed response when an abrupt load is added in case of the two controllers. When load abruptly changes, the adaptive NTSMC with DOB shows better robustness. Speed fluctuation of the control system under the NTSM with DOB technique is smaller, and the recovering time against disturbance is shorter. Fig.12 shows the response of the current when a sudden load is added. Here, the excitation current is set as 0.5A with external torque equal to rated load. It can be seen clearly that the adaptive NTSM with DOB method is able to track currents well with less time, smaller overshoot and better robustness

In order to better illustrate the superiority of the proposed algorithm, this paper introduces some control system performance indexes, such as overshoot (OS%), settling

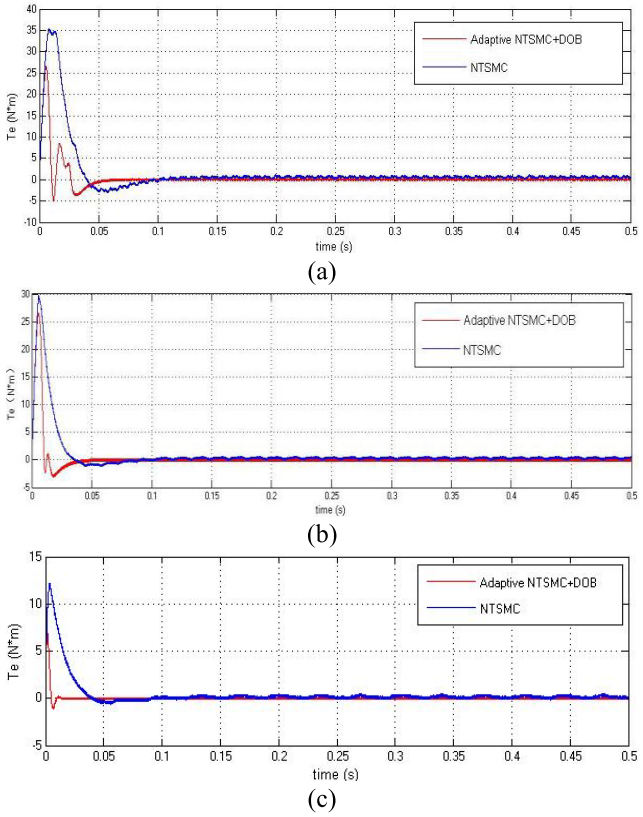

FIGURE 9. Torque responses under the control of the adaptive NTSMC with DOB and NTSMC (a) 1200r/min (b) 600r/min (c) 300r/min.

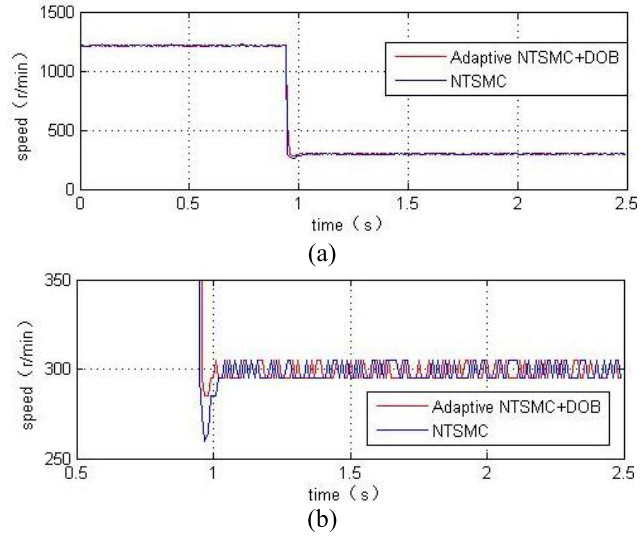

FIGURE 10. Speed responses with a sudden change of speed from 1200r/min to 300r/min under the control of the adaptive NTSMC with DOB and NTSMC (a) Speed responses curve (b) Local curve zoom.

time (t_s) and maximum decrease of speed caused by load torque. TABLE 1 demonstrates the comparison of performance indexes from the two methods under different conditions. It can be observed accurately that in all three aspects the adaptive NTSMC with DOB has a better performance

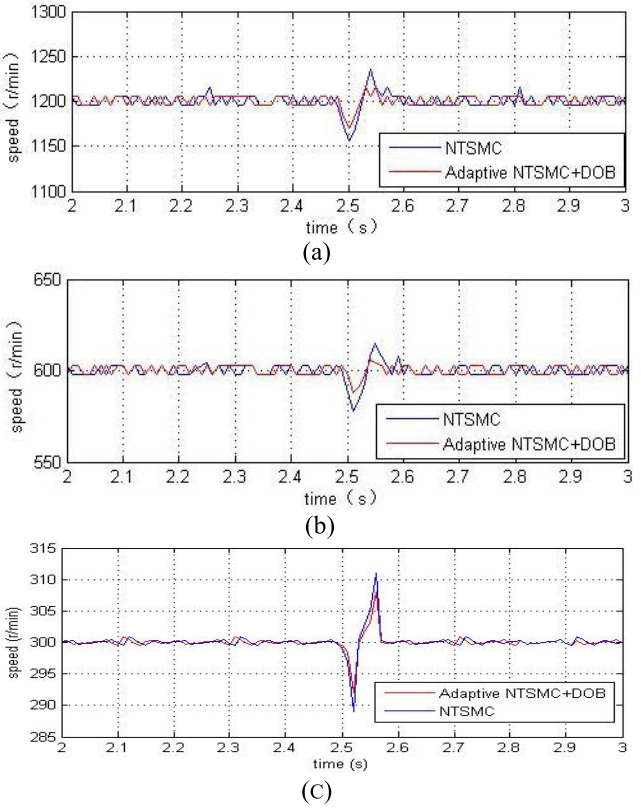

FIGURE 11. Speed responses of a sudden load under the control of the adaptive NTSMC with DOB and NTSMC (a) 1200r/min (b) 600r/min (c) 300r/min.

TABLE 1. Comparison of the major performance indices.

Control scheme \ Index		OS (%)	t_s/(ms)	Speed decrease/ (rpm)
300r/min	NTSMC	3.12	61	11
	adaptive NTSMC+DOB	2.3	19	8
600r/min	NTSMC	5.33	80	21
	adaptive NTSMC+DOB	2.17	25	12
1200r/min	NTSMC	1.33	70	46
	adaptive NTSMC+DOB	0.42	40	30

than NTSMC, and its response time is 42.86%, 68.75% and 68.85% respectively at 300r/min, and 600 r/min and 1200r/min, faster than NTSM. In addition, its overshoot is smaller. As shown in TABLE 2, with speed changing from 1200r/min to 300r/min, the adaptive NTSMC with DOB precisely tracks it with less time.

The experimental results show that the design of the new type of disturbance observer based terminal sliding mode control, applied to PMSM vector control speed regulation system is effective and feasible. It can not only well ensure the dynamic performance of the PMSM speed control system, but

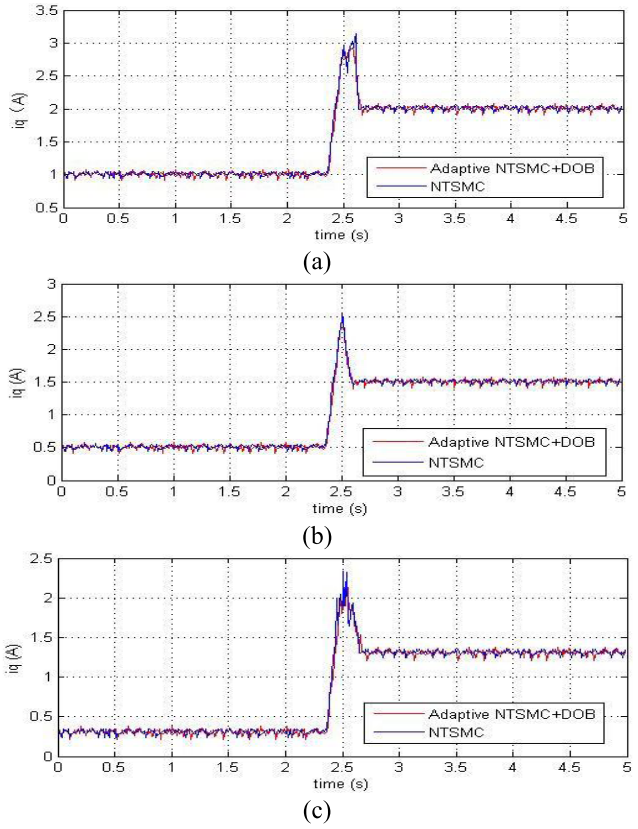

FIGURE 12. Current responses of a sudden load under the control of the adaptive NTSMC with DOB and NTSMC (a) 1200r/min (b) 600r/min (c) 300r/min.

TABLE 2. Speed change.

Control scheme \ Index		OS（%）	t/(ms)
1200r/min to 300r/min	NTSMC	14.67	5
	adaptive NTSMC+DOB	4.33	3

also can effectively improve system robustness and weaken system chattering.

VI. CONCLUSIONS

In this paper, an adaptive nonsingular terminal sliding model control with disturbance observer is presented for PMSM system. The combination of the adaptive NTSMC and disturbance observer not only shortens system response time but also improves system robustness. The simulation and experimental results indicate that the proposed method has rapid and higher robustness, making lower chattering and improving system efficiency.

REFERENCES

[1] S. Li and Z. Liu, "Adaptive speed control for permanent-magnet synchronous motor system with variations of load inertia," *IEEE Trans. Ind. Electron.*, vol. 56, no. 8, pp. 3050–3059, Aug. 2009.

[2] S. Li, M. Zhou, and X. Yu, "Design and implementation of terminal sliding mode control method for PMSM speed regulation system," *IEEE Trans. Ind. Informat.*, vol. 9, no. 4, pp. 1879–1891, Nov. 2013.

[3] G.-J. Wang, C.-T. Fong, and K. J. Chang, "Neural-network-based self-tuning PI controller for precise motion control of PMAC motors," *IEEE Trans. Ind. Electron.*, vol. 48, no. 2, pp. 408–415, Apr. 2001.

[4] M. N. Uddin, M. A. Abido, and M. A. Rahman, "Development and implementation of a hybrid intelligent controller for interior permanent-magnet synchronous motor drives," *IEEE Trans. Ind. Appl.*, vol. 40, no. 1, pp. 68–76, Jan./Feb. 2004.

[5] Q. Sun, M. Cheng, and E. Zhou, "Variable PI control of a novel doubly salient permanent magnet motor drive," *Proc. CSEE*, vol. 23, no. 6, pp. 117–123, Jun. 2003.

[6] H. H. Choi, N. T.-T. Vu, and J.-W. Jung, "Digital implementation of an adaptive speed regulator for a PMSM," *IEEE Trans. Power Electron.*, vol. 26, no. 1, pp. 3–8, Jan. 2011.

[7] H. B. Wang, B. Zhou, and S. C. Fang, "A PMSM sliding-mode control system based-on exponential reaching law," *Trans. China Electrotech. Soc.*, vol. 24, no. 9, pp. 71–77, Sep. 2009.

[8] F. F. M. El-Sousy, "Hybrid H-infinity-based wavelet-neural-network tracking control for permanent-magnet synchronous motor servo drives," *IEEE Trans. Ind. Electron.*, vol. 57, no. 9, pp. 3157–3166, Sep. 2010.

[9] R. Errouissi, M. Ouhrouche, W.-H. Chen, and A. M. Trzynadlowski, "Robust nonlinear predictive controller for permanent-magnet synchronous motors with an optimized cost function," *IEEE Trans. Ind. Electron.*, vol. 59, no. 7, pp. 2849–2858, Jul. 2012.

[10] Y. Luo, Y. Chen, H.-S. Ahn, and Y. Pi, "Fractional order robust control for cogging effect compensation in PMSM position servo systems: Stability analysis and experiments," *Control Eng. Pract.*, vol. 18, no. 9, pp. 1022–1036, Sep. 2010.

[11] X. Sun, Z. Shi, L. Chen, and Z. Yang, "Internal model control for a bearingless permanent magnet synchronous motor based on inverse system method," *IEEE Trans. Energy Convers.*, vol. 31, no. 4, pp. 1539–1548, Dec. 2016.

[12] W. Ji, G. Shi, B. Xu, and J. Xu, "An improved rotating HF signal injection method based on FIR filters for state estimation of BPMSM sensorless control," *Adv. Mech. Eng.*, vol. 9, no. 12, pp. 1–10, Dec. 2017.

[13] J. Yang, S. Li, and X. Yu, "Sliding-mode control for systems with mismatched uncertainties via a disturbance observer," *IEEE Trans. Ind. Electron.*, vol. 60, no. 1, pp. 160–169, Jan. 2013.

[14] S. Ding and S. Li, "Second-order sliding mode controller design subject to mismatched term," *Automatica*, vol. 77, no. 3, pp. 388–392, Mar. 2017.

[15] A. Sabanovic, "Variable structure systems with sliding modes in motion control—A survey," *IEEE Trans. Ind. Informat.*, vol. 7, no. 2, pp. 212–223, May 2011.

[16] S. Ding, W. Zheng, J. Sun, and J. Wang, "Second-order sliding-mode controller design and its implementation for buck converters," *IEEE Trans. Ind. Informat.*, vol. 14, no. 5, pp. 1990–2000, May 2018, doi: 10.1109/TII.2017.2758263.

[17] M. Zak, "Terminal attractors in neural networks," *Neural Netw.*, vol. 2, no. 4, pp. 259–274, 1989.

[18] S. Li, H. Du, and X. Yu, "Discrete-time terminal sliding mode control systems based on Euler's discretization," *IEEE Trans. Autom. Control*, vol. 59, no. 2, pp. 546–552, Feb. 2014.

[19] Y. Feng, X. Yu, and Z. Man, "Non-singular terminal sliding mode control of rigid manipulators," *Automatica*, vol. 38, no. 12, pp. 2159–2167, Dec. 2002.

[20] Y. Feng, J. Zheng, X. Yu, and N. V. Truong, "Hybrid terminal sliding-mode observer design method for a permanent-magnet synchronous motor control system," *IEEE Trans. Ind. Electron.*, vol. 56, no. 9, pp. 3424–3431, Sep. 2009.

[21] K.-W. Tong, X. Zhang, and Y. Zhang, "Sliding mode variable structure control of permanent magnet synchronous machine based on a novel reaching law," *Proc. CSEE*, vol. 28, no. 21, pp. 102–106, Jul. 2008.

[22] B. Xu, G. D. Shi, W. Ji, F. Y. Liu, S. H. Ding, and H. Q. Zhu, "Design of an adaptive nonsingular terminal sliding model control method for a bearingless permanent magnet synchronous motor," *Trans. Inst. Meas. Control*, vol. 39, no. 12, pp. 1821–1828, Dec. 2017.

[23] B. Xu, F. Mu, G. Shi, W. Ji, and H. Zhu, "State estimation of permanent magnet synchronous motor using improved square root UKF," *Energies*, vol. 9, no. 7, p. 489, Jul. 2016.

[24] X. J. Wei and L. Guo, "Composite disturbance-observer-based control and H_∞ control for complex continuous models," *Int. J. Robust Nonlinear Control*, vol. 20, no. 1, pp. 106–118, Jan. 2010.

[25] X.-J. Wei, Z.-J. Wu, and H. R. Karimi, "Disturbance observer-based disturbance attenuation control for a class of stochastic systems," *Automatica*, vol. 63, pp. 21–25, Jan. 2016.
[26] J. Xu, B. Xu, W. Ji, G. Shi, and S. Ding, "Research on speed sensorless operation of PMSM based on improved MRAS," in *Proc. 11th Asian Control Conf. (ASCC)*, Dec. 2017, pp. 1423–1427.

BO XU was born in Xuzhou, Jiangsu, China, in 1977. She received the B.Sc. degree in automatic control from the China University of Mining and Technology, Xuzhou, in 1999, and the M.Sc. degree in computer science and the Ph.D. degree in electrical engineering from Jiangsu University, Zhenjiang, China, in 2005 and 2012, respectively.

Since 1999, she has been with the School of Electrical and Information Engineering, Jiangsu University, where she is currently an Associate Professor. Her current research interests include motor sensorless control and intelligent control.

XIAOKANG SHEN was born in Huaian, Jiangsu, China, in 1993. He received the B.Sc. degree in electrical and electronic engineering from the Huaiyin Institute of Technology, Zhenjiang, China, in 2017.

He is currently pursuing the M.Sc. degree with the School of Electrical and Information Engineering, Jiangsu University, Zhenjiang. His research interests include motor drive and control and intelligent control.

WEI JI was born in Zhoukou, Henan, China, in 1974. He received the B.Sc. and M.Sc. degrees in electrical engineering from the China University of Mining and Technology, Xuzhou, China, in 1999 and 2002, respectively, and the Ph.D. degree in electrical engineering from Southeast University, Nanjing, China, in 2007.

Since 2007, he has been with the School of Electrical and Information Engineering, Jiangsu University, Zhenjiang, China, where he is currently an Associate Professor. His current research interests include robot motion control and intelligent control.

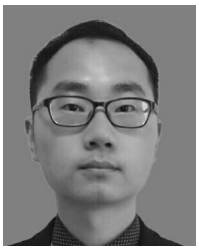

GUODING SHI was born in Nanjing, Jiangsu, China, in 1992. He received the B.Sc. degree in electrical and electronic engineering from Jiangsu University, Zhenjiang, China, in 2015.

He is currently pursuing the M.Sc. degree with the School of Electrical and Information Engineering, Jiangsu University. His research interests include motor drive and control and intelligent control.

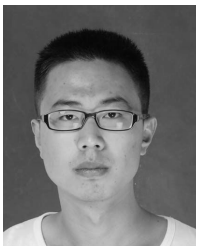

JIAN XU was born in Tongling, Anhui, China, in 1994. He received the B.Sc. degree in electrical and electronic engineering from Tongling University, Tongling, in 2016.

He is currently pursuing the M.Sc. degree with the School of Electrical and Information Engineering, Jiangsu University, Zhenjiang, China. His research interests include motor control and intelligent control.

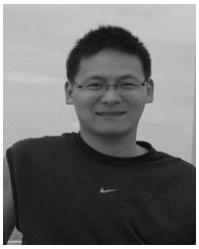

SHIHONG DING was born in Maanshan, Anhui, China, in 1983. He received the B.E. degree in mathematics from Anhui Normal University, China, in 2004, and the M.S. degree and the Ph.D. degree in automatic control from Southeast University, China, in 2007 and 2010, respectively. During his graduate studies, he visited The University of Texas at San Antonio from 2008 to 2009. Upon graduation, he has held a Research Fellowship with the University of Western Sydney.

He is currently a Professor with the School of Electrical and Information Engineering, Jiangsu University. His current research interests include sliding mode control and finite-time stability.